Elsevier Editorial System(tm) for Electrochimica Acta

Manuscript Draft

Manuscript Number: AMPT15-36R1

Title: A Polyketone based Anion-Exchange Membrane for Electrochemical Applications: Synthesis and Characterization

Article Type: SI: AMPT 2015 Madrid

Keywords: Polyketone, Polyamines, Anion-exchange membrane, Conductivity

Corresponding Author: Professor. rosa di maggio,

Corresponding Author's Institution: University of Trento

First Author: rosa di maggio

Order of Authors: rosa di maggio; Narges Atahollahi; Keti Vezzù, PhD; Graeme Nawn, PhD; Giuseppe Pace, PhD; Gianni Cavinato, professor; Fabrizio Girardi, PhD; Paolo Scardi, Full professor; Vito Di Noto, full professor

Manuscript Region of Origin: ITALY

Abstract: An anion exchange membrane (AEM) was made of modified polyketone (PK) in order to avoid the use of expensive materials. AEMs of polyamines were prepared according to a three steps procedure: (i) synthesis of PK using ethylene and carbon monoxide assisted by Pd catalyst, followed by the introduction of 1,2-diaminopropane to yield the polymeric amines; (ii) solvent casting of modified PK with low degree of amination to form a membrane; (iii) iodomethylation to form AEM (PK-PDAPm(I)), followed by ion exchange with KOH (PK-PDAPm(OH)).
The structure of modified polyketone was characterized by FTIR and further supported by UV-Vis spectroscopy, demonstrating the successful introduction of amine into PK. Conductivity of AEM was studied by broadband electric spectroscopy (BES) in the temperature range from -100 to 120 °C, showing the highest value of 9 x 10-4 S·cm-1 at 120 °C for the ionic conductivity of PK-PDAPm(I) followed by PK-PDAPm(OH) with values within the same order of magnitude (10-4 S·cm-1). Thermogravimetry revealed that this material is thermally stable up to 200 °C, further confirming the modified polyketone AEM as a promising candidate for electrochemical applications.

Table 1. Composition of the samples

Sample	**%C***	**%H***	**%O[#]**	**%N***	**%I[§]**	**nC**	**nH**	**nO**	**nN**	**nI**	**nH/nC**	**nO/nC**	**nI/nN**
Theoretical PK	64.27	7.19	28.54	/	/	3.00	4.00	1.00	/	/	1.333	0.333	/
PK	61.83	7.17	31.00	/	/	5.15	7.11	1.94	/	/	1.382	0.376	/
PK-PDAP	62.00	7.34	25.32	5.34	/	5.16	7.28	1.58	0.381	/	1.411	0.307	/
PK-PDAPm	60.57	8.07	25.55	5.81	/	5.04	8.01	1.60	0.415	/	1.588	0.317	/
PK-PDAPm(I)	62.01	7.54	19.41	5.96	5.08	5.16	7.48	1.21	0.426	0.04	1.449	0.235	0.094
PK-PDAPm(OH)	60.73	7.92	25.63	5.72	/	5.06	7.86	1.60	0.408		1.554	0.0317	/

* determined by elemental analyses and § ICP measurements; [#] **%O** is obtained as difference to 100

Table 2. FT-IR peak observation of pristine PK, PK-PDAP, PK-PDAPm, PK-PDAPm(I) and PKPDAPm(OH). Assignments have been performed correlatively.

Continued

Wavenumber (cm^{-1}) & intensity					Band assignment	Reference
PK	**PK-PDAP**	**PK-PDAPm**	**PK-PDAPm(I)**	**PK-PDAPm(OH)**		
466 (vw)	466(vw)	462 (vw)	463(vw)	462 (vw)	δ(CCC)	[37,44]
543 (vw)	541(vw)	539 (vw)	539 (vw)	538 (vw)	δ (CC=O)	[37,42,44]
591 (w)	590 (w)	592 (vw)	592 (vw)	592 (vw)	δ(C=O) in-plane	[37,42,44]
666 (vw)	665 (vw)	663 (vw)	665 (vw)	668 (vw)	*v* (CH_2)	[42]
			684 (vw)	684 (vw)	*v* (C-N)	[45]
		726 (vw)	726 (vw)	725 (vw)	δ (CH_2) long-chain band	[45]
	754 (vw)	770 (vw)	774 (vw)	768 (vw)	(C-C) oop of ring	[35,44,47]
810 (vw)	808 (vw)	808 (vw)	807 (vw	807 (vw)	} *p* (CH_2)	[37,42,43]
831 (sh,vw)	831(sh,vw)	833 (sh,vw)	836 (sh,vw)	830 (sh,vw)		
	919 (vw)		890 (vw)	917 (vw)	} δ (=C-H) oop	[45]
		954 (vw)	954 (vw)	952 (vw)		
			970 (vw)	970 (vw)		
1055 (w)	1056 (w)	1054 (vw)	1054 (vw)	1054 (vw)	w (CH_2)	[37]
	1076 (sh,vw)	1072 (sh,vw)	1072 (sh,vw)	1070 (sh,vw)	*v* (C-N)	[44,45]
			1095 (sh,vw)	1089(vw)	*v* (C-N)	[44,45]

Wavenumber (cm^{-1}) & intensity					Band assignment	Reference
PK	**PK-PDAP**	**PK-PDAPm**	**PK-PDAPm(I)**	**PK-PDAPm(OH)**		
		1173 (vw)	1174 (vw)	1175 (vw)	*v* (C-N)	[44,45]
		1217(vw)	1213 (vw)	1216 (vw)	*v* (C-N)	[44,45]
1258 (vw)	1259 (vw)	1258 (vw)	1258 (vw)	1258 (vw)	δ (CH_2)	[37,40,41,43]
	1296 (sh,vw)		1282 (sh,vw)	1291 (sh,vw)	*v* (C-N)	[44,45]
1331 (w)	1330 (w)	1330 (v)	1331(vw)	1331(vw)	*w* (CH_2)	[40,41,42]
1351 (sh,vw)	1353 (sh,vw)	1351(sh,vw)	1352(sh,vw)	1351(sh,vw)	δ(CH_3) *sym*	[45]
1405 (w)	1405 (w)	1405 (vw)	1405 (vw)	1405 (vw)	*v* (CH_2)	[40,41, 42]
1427 (sh,vw)	1427(sh,vw)	1426 (sh,vw)	1426 (sh,vw)	1424 (sh,vw)	δ(CH_3)	[42]
	1567 (b,vw)	1557 (vw)	1558 (vw)	1559 (vw)	} *v* (C=C) of ring	[47]
			1590 (vw)	1590 (vw)		
1662 (sh,vw)	1662 (sh,vw)	1663 (sh,vw)	1662 (sh,vw)	1662 (sh,vw)	*v* (C=C)	[37,44]
1688 (vs)	1689 (m)	1689 (vw)	1689 (w)	1689 (vw)	*v* (C=O)	[37-41]
2911(vw)	2912 (vw)	2910 (vw)	2910 (vw)	2908 (vw)	*v* (CH_2) *sym*	[37,42,44]
2947 (sh,vw)	2966 (sh,vw)	2951 (sh,vw)	2951 (sh,vw)	2946 (sh,vw)	*v* (CH_2) *asym*	[37,44,45]
3390 (vw)	3386 (vw)	3360 (vw)	3387 (vw)	3381(vw)	*v*(OH)	[37,42,44,46]

Relative intensities are reported in parentheses: *vs*: very strong; *s*: strong; *m*: medium; *w*: weak; *vw*: very weak; *sh*: shoulder. *v*: stretching; δ: bending; *w*: wagging; *p*: rocking; b: broad; oop: out-of- plane; *asym:* antisymmetric mode*; sym:* symmetric.

Table 3. Activation energy of overall conductivity (σ_T) in the four conductivity regions for dry and wet membranes (PK-PDAPm(I) and PK-PDAPm(OH)).

	Sample	**I**	**II**		**III**		**IV**	
		E_a/ kJ/mol	**E_a/** kJ/mol	**T_0 /K**	**E_a/** kJ/mol	**T_0/K**	**E_a/** kJ/mol	**T_0/K**
dry	I	4.44±0.38*	80.91 ±4.11*	/	1.23±0.11°	183±9	/	/
	OH	11.21±1.32*	136.7±8.31*	/	2.24±0.08°	172±9	51.02±3.06*	/
wet	I	33.03±2.09*	0.272±0.042°	197±10	3.80±0.23°	197±8	5.29±0.48°	197±6
	OH	33.08±3.01*	0.305±0.039°	187±8	1.94±0.31°	187±9	1.09±0.06°	197±5

* The value of E_a is determined by fitting the conductivity data with Arrhenius equation.
° The value of E_a is obtained by fitting the conductivity data with VTF equation.

Figure(s)

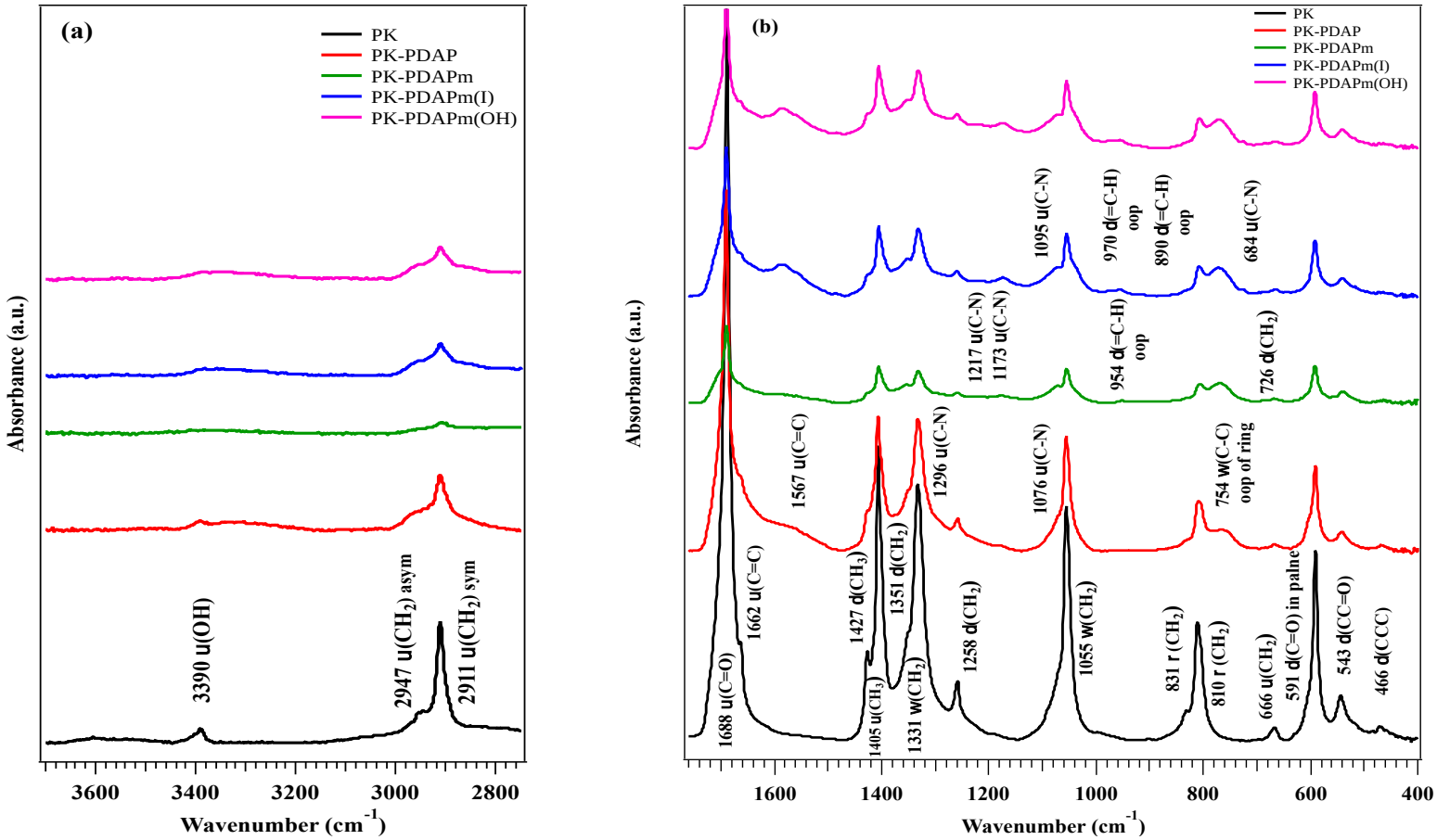

Figure 1. IR spectra of pristine PK, PK-PDAP, PK-PDAPm, PK-PDAPm(I) and PKPDAPm(OH)

(a) in the range of 3700-2750 cm^{-1} and (b) in the range of 1750-400 cm^{-1}

(*v*: stretching; δ: bending; *w*: wagging; *p*: rocking; b: broad; oop: out-of- plane; *asym:* antisymmetric mode*; sym:* symmetric mode)

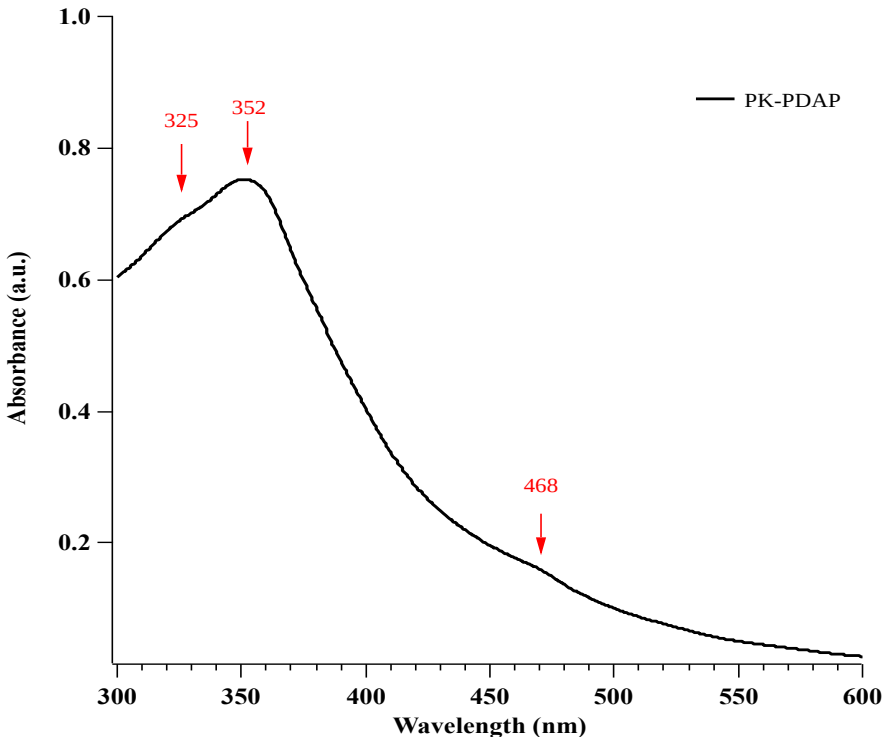

Figure 2: UV-Vis spectrum of PK-PDAP at 300-600 nm

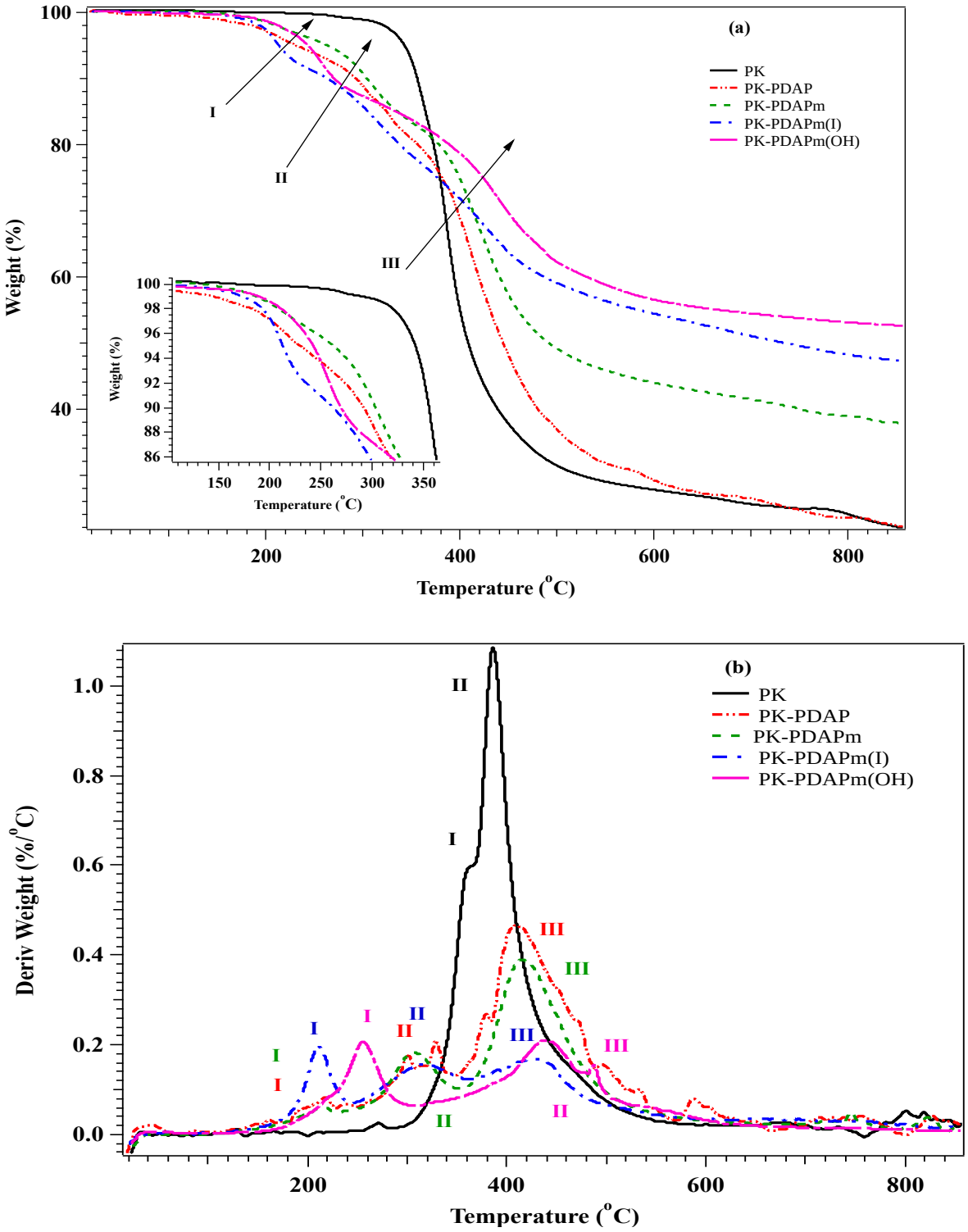

Figure 3. a) TGA profiles and b) The dependence of the derivative of TG profile on temperature of PK, PK-PDAP, PK-PDAPm, PK-PDAPm(I) and PK-PDAPm(OH)

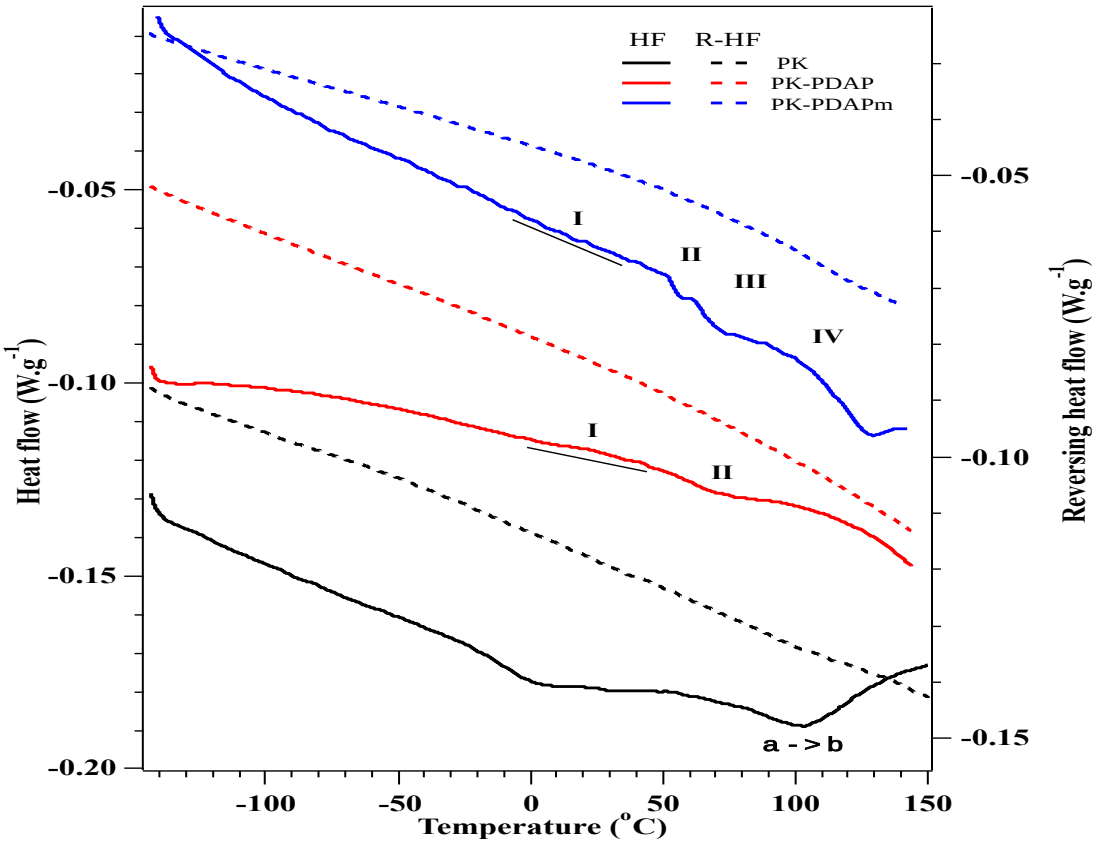

Figure 4. mDSC profile of PK, PK-PDAP and PK-PDAPm in dry condition

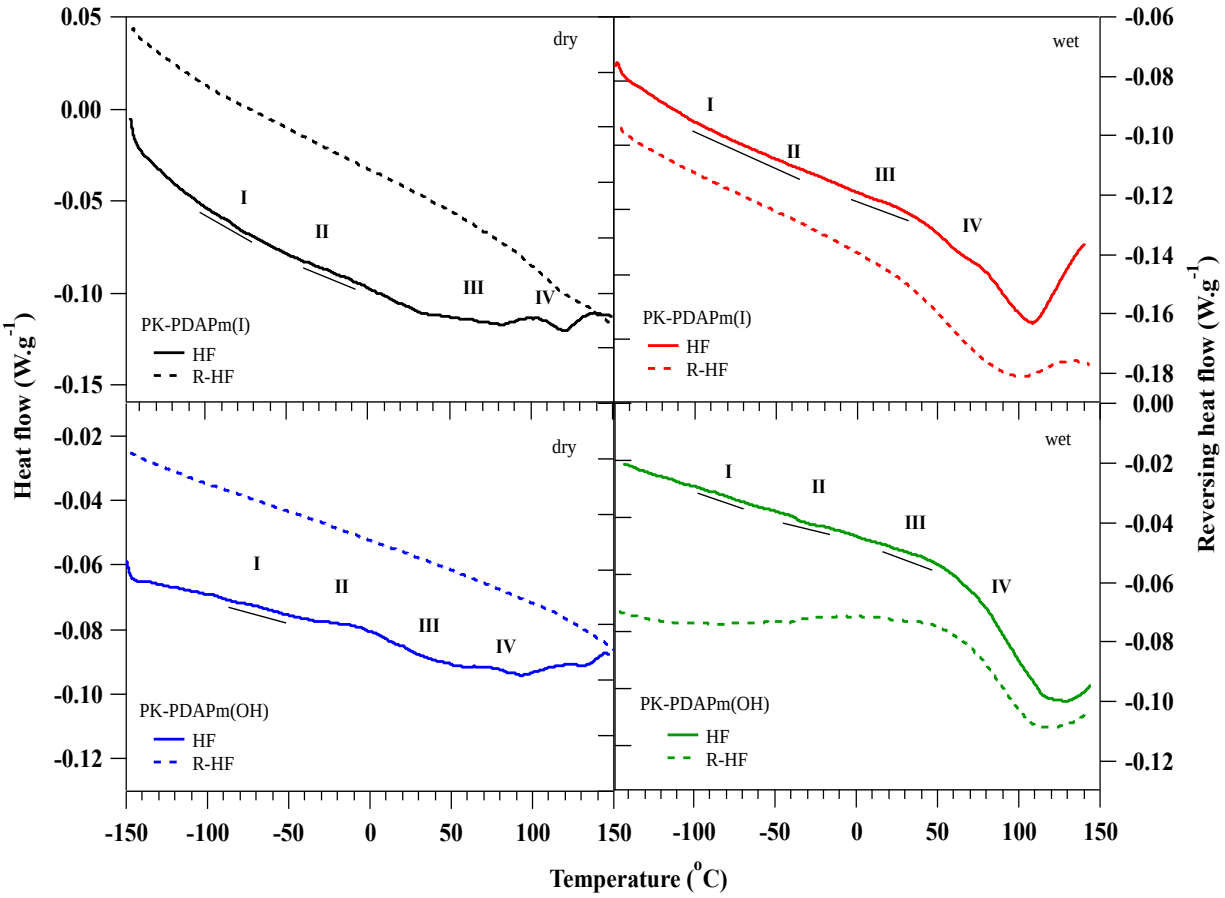

Figure 5. mDSC profile of PK-PDAPm(I) and PK-PDAPm(OH) in dry and wet condition

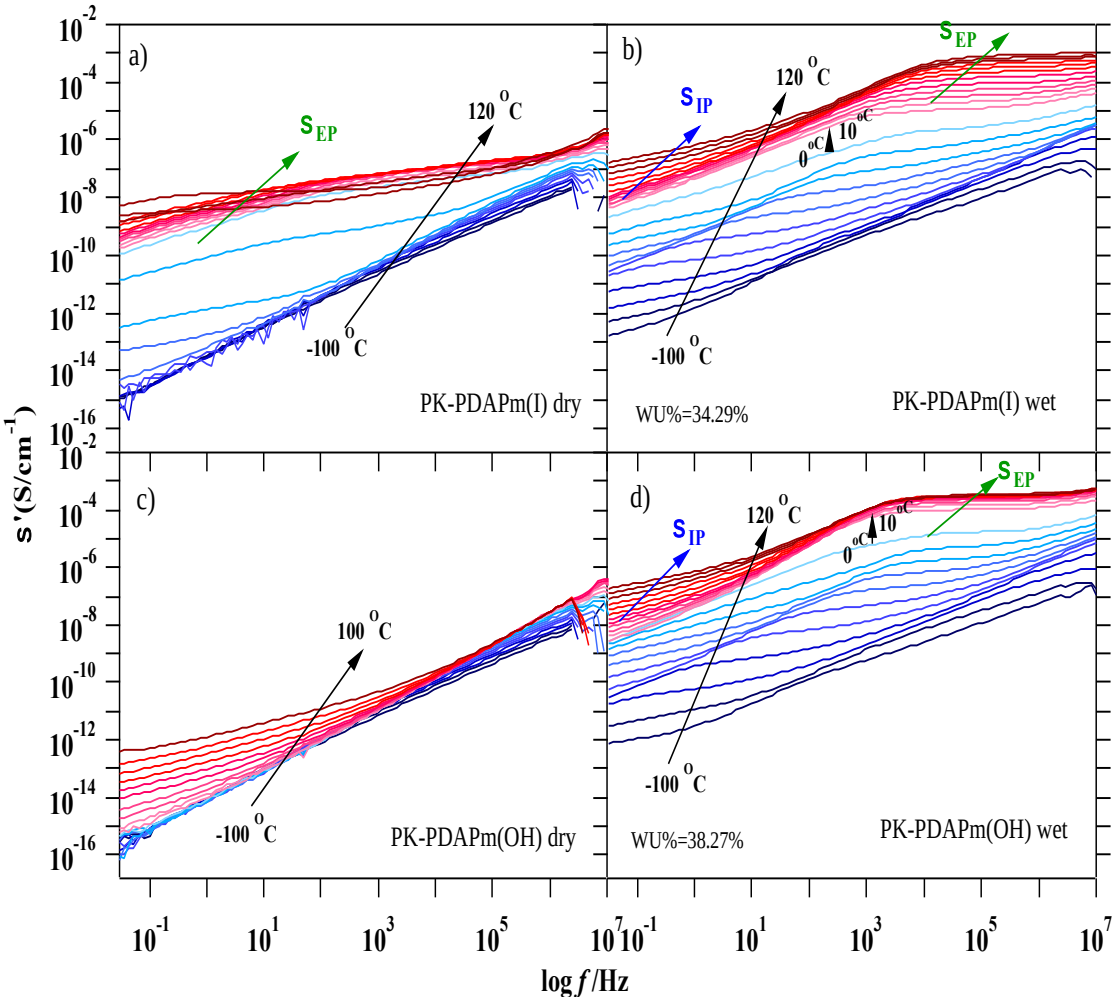

Figure 6. Real conductivity as a function of frequency and temperature for dry (a,c) and wet (b,d) iodide (a,b) and OH (c,d) conducting membrane. The black lines refer to change of temperature from -100 to 120 ^{o}C, the blue lines to the σ_{IP} and the green to the σ_{EP}

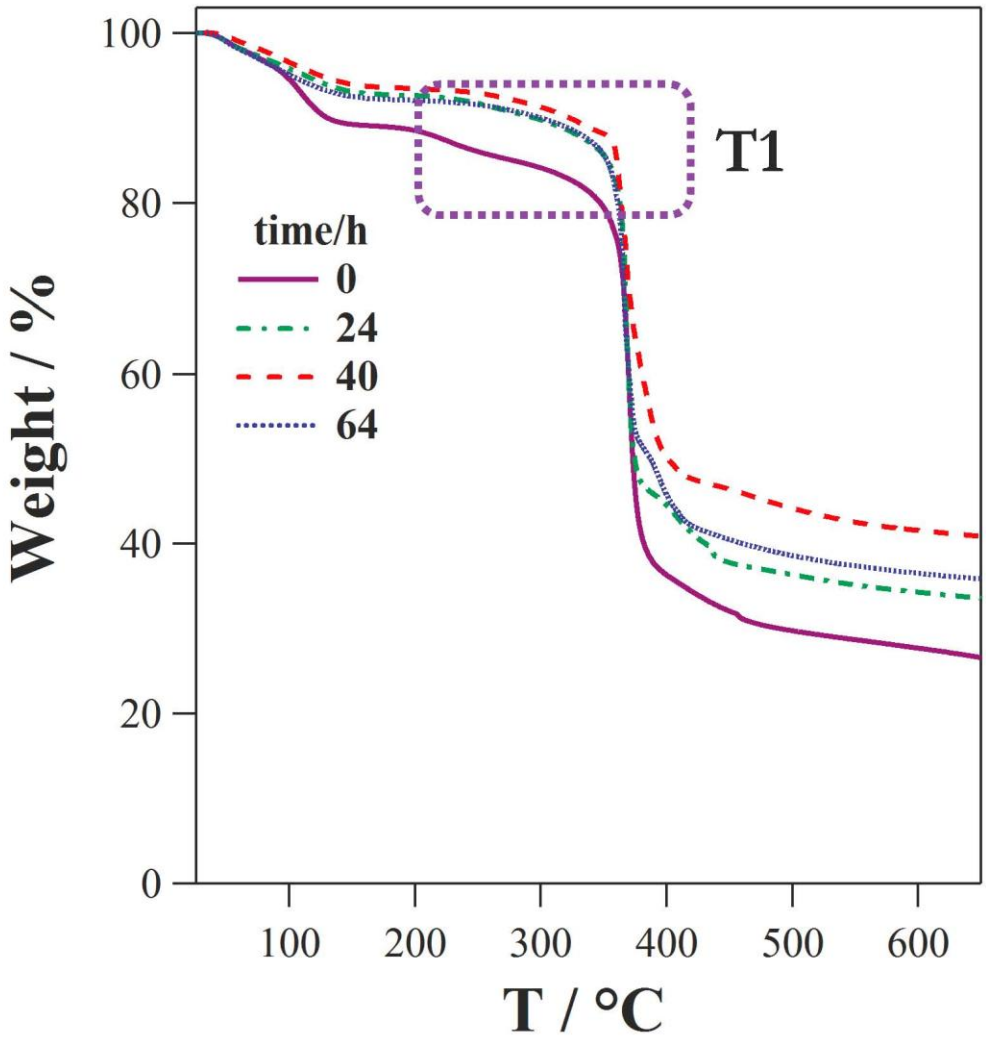

Figure 7a. Thermogravimetric curve of weight loss vs. temperature of PK-PDAPm(OH) samples immersed into a 2M NaOH solution at 80°C for increasing times.

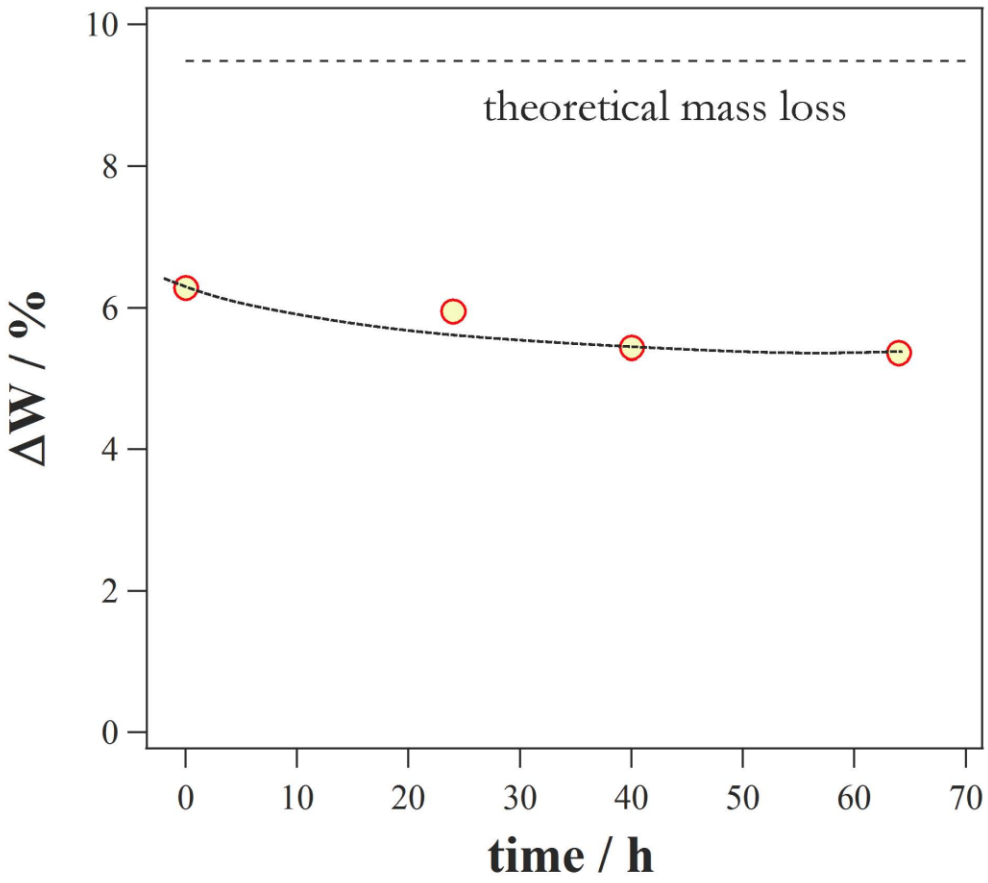

Figure 7b. Weight loss variation vs. times of immersion of PK-PDAPm(OH) samples immersed into a 2M NaOH solution.

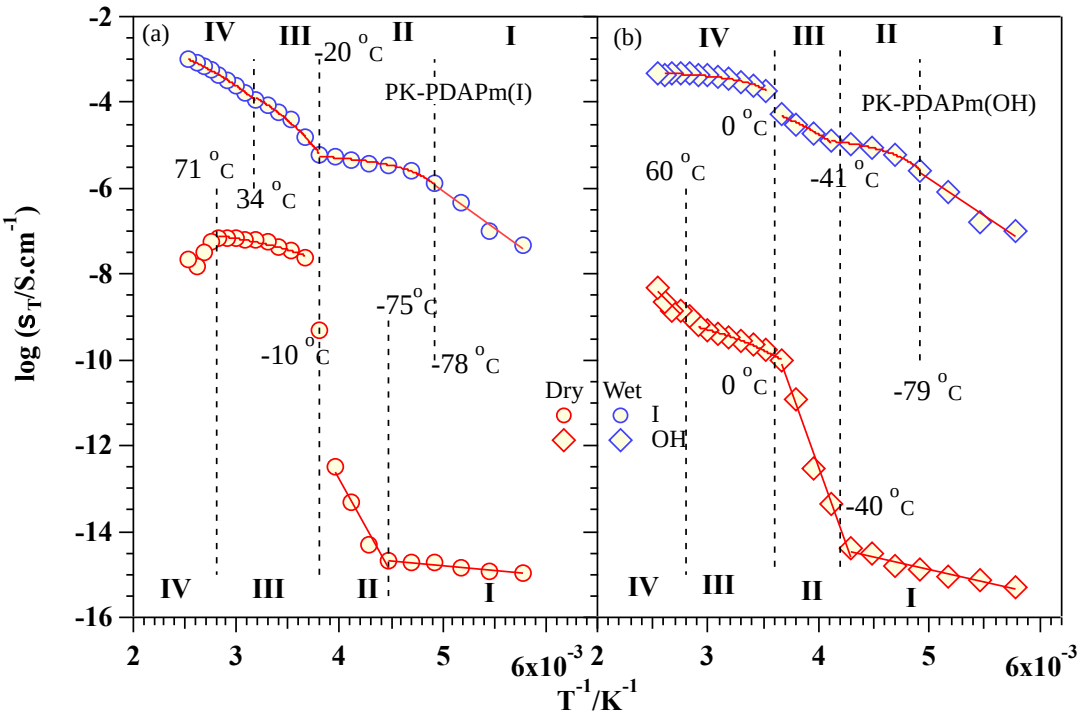

Figure 8. Conductivity vs 1/T for dry and wet PK-PDAPm(I) (a) and PK-PDAPm(OH) (b). Four conductivity regions are detected (I, II, III, & IV) and defined by temperature of mDSC.

Supplementary Materials

Click here to download Supplementary Materials: Electrochimica Acta_DiMaggio_SI_revised.doc

A Polyketone based Anion-Exchange Membrane for electrochemical applications: Synthesis and Characterization

Narges Ataollahi[a], Keti Vezzù[b], Graeme Nawn[b], Giuseppe Pace[c], Gianni Cavinato[d], Fabrizio Girardi[a], Paolo Scardi[a],Vito Di Noto[b,c,*], Rosa Di Maggio[a,*]

[a]Department of Civil, Environmental and Mechanical Engineering, University of Trento, Via Mesiano, 77, 38123, Trento, Italy
[b] Section of Chemistry for Technology, Department of Industrial Engineering, University of Padova, Via Marzolo 9, I-35131 Padova, Italy
[c]Istituto di Chimica della Materia Condensata e di Tecnologie per l'Energia (CNR-ICMATE), Via Marzolo1, I35131 Padova (PD), Italy
[d]Department of Chemical Sciences, University of Padova,
Via Marzolo1, I35131 Padova (PD), Italy

Corresponding author:
[*] *vito.dinoto@unipd.it*, *rosa.dimaggio@unitn.it*

Abstract

An anion exchange membrane (AEM) was made of modified polyketone (PK) in order to avoid the use of expensive materials. AEMs of polyamines were prepared according to a three steps procedure: (i) synthesis of PK using ethylene and carbon monoxide assisted by Pd catalyst, followed by the introduction of 1,2-diaminopropane to yield the polymeric amines; (ii) solvent casting of modified PK with low degree of amination to form a membrane; (iii) iodomethylation to form AEM (PK-PDAPm(I)), followed by ion exchange with KOH (PK-PDAPm(OH)).

The structure of modified polyketone was characterized by FTIR and further supported by UV-Vis spectroscopy, demonstrating the successful introduction of amine into PK. Conductivity of AEM was studied by broadband electric spectroscopy (BES) in the temperature range from -100 to 120 °C, showing the highest value of 9 x 10^{-4} $S \cdot cm^{-1}$

at 120 °C for the ionic conductivity of PK-PDAPm(I) followed by PK-PDAPm(OH) with values within the same order of magnitude (10^{-4} $S \cdot cm^{-1}$). Thermogravimetry revealed that this material is thermally stable up to 200 °C, further confirming the modified polyketone AEM as a promising candidate for electrochemical applications.

Keywords: Polyketone, Polyamines, Anion-exchange membrane, Conductivity

1. Introduction

Anion exchange membranes (AEMs) have shown promising characteristics to overcome some of the problems associated with cation exchange membranes [1-6] and are key components of various electrochemical devices. Among the potential applications, electrochemical energy conversion [7], storage systems [8], electrolyzers [9] and even electro-dialysis for water desalination [10] are some of the most important and well-known. The selective transport anionic charge carriers, lower crossover of cationic redox couples, and facile reaction kinetics in energy conversion processes of AEMs result mainly from the density and distribution of positively charged functional groups, along with a macromolecular polymer backbone. As a result, there has been an increasing demand for the development of AEMs with better selectivity, higher chemical stability and conductivity, and a lot of work has been carried out in this area. High mechanical properties, good dimensional stability, high hydroxide conductivity and stability are key properties for an anion exchange membrane. However, despite efforts devoted to the fabrication of high-performance AEMs, it is very difficult to simultaneously maximize all of them. The polymer electrolyte membrane is usually made of positively charged groups fixed to the backbone of the polymer (typically quaternary ammonium functional group), which allows the transfer of anions such as I^-, Cl^-, Br^- and OH^-.

However, the challenge is to develop an anion exchange membrane [11-15] having not only high thermal and mechanical performance, but also OH^- ion conductivity comparable to that observed for H^+ in proton exchange membrane (PEM). Accordingly, enough ion-conducting groups (typically quaternary ammonium groups) need to be attached onto the main chain of the polymer in order to reach high hydroxide

conductivity. The quaternary ammonium ionic groups are less dissociated compared to sulfonic acid ones, in addition the hydroxide ions have lower diffusion coefficient, leading to lower conductivity compared to PEM. To achieve similar results, higher concentration of OH^- is required. Hence, various types of membranes were developed including membrane based on polymerization [16], chemical grafting [17] radiation-induced grafting, and copolymerization [18,19]. Chemical modification into a polymer is also considered as a suitable method to obtain AEMs [20]. However, the main issue in this method is how to introduce the functional group and chloromethylmethyl ether is often used in this approach [21].

The aim of this study is to prepare a new anion exchange membrane based on polyamine. Polyketone is obtained from reaction of ethylene and carbon monoxide in the presence of palladium catalyst [22]. The synthesis was first reported in 1941 [23] and thereafter the production of PK became popular among academic and industrial areas. Low-cost and easy availability of ethylene and carbon monoxide [24,25] further contributed to increase the production of PK. In addition, this polar polymer has a desirable set of properties such as excellent mechanical properties, resistance against pressure and heat [26], chemical resistance to acids, bases and solvents [27] as well as high rigidity, impact strength and stability against electrolytic corrosion [28]. Moreover, PK is very attractive because its functional properties can be potentially modulated, by changing carbonyls into a wide variety of other functional groups [29-32].

In this study the reaction of 1,4-dicarbonyl moieties of PK with primary amine leads to the formation of a N-substituted pyrrole unit. This occurs under mild condition without using any solvent. The chemical modification is an easy and simple route,

leading to the creation of a new polymer with a stable pyrrole ring along the backbone, and a reactive pendant amino functional group [33-35], which allows for the introduction of quaternary ammonium cation groups with iodomethane, followed by OH^- ion exchange processes. The properties of modified PK thus obtained can fulfill the thermal and chemical properties typically required for an anionic membrane.

2. Experimental

2.1 Reagents

1,2-diaminopropane (99%), 1,1,1,3,3,3,-hexafluoroisopropanol (99%), 1,3-bis (diphenylphosphino) propane [dppp] (97%), diethyl ether (99.8%), methanol (99.8%), petroleum ether (95%) and trimethylamine (99%) have been purchased from Sigma-Aldrich. Potassium hydroxide obtained from VWR. *p*-toluene-sulfonic acid [*p*-TsOH] (99%) was purchased from ACROS. Ammonium hydroxide (28-30 %) was obtained from J.T. Baker and iodomethane (99%) was purchased from ABCR GmbH. Carbon monoxide (N37) (99.97%) and ethylene (N25) (99.5%) were supplied from Air Liquid company. Bi-distilled water was used in all procedures. All the reagents and solvents were used as received.

2.2 Synthesis of Polyketone

The reaction was carried out in a 250 mL Hastelloy C stainless steel autoclave equipped with a self-aspirating turbine using a 150 mL Pyrex glass beaker to avoid contamination from metallic species. The [Pd(*p*-TSO)(H_2O)(DPPP)] *p*-TSO catalyst is prepared as described in the literature [36,37].

In a 150 mL Pyrex glass beaker, 10 mg of catalyst [Pd(*p*-TSO)(H_2O)(DPPP)] *p*-TSO (0.011 mmol), 20 mg *p*-TsOH (0.10 mmol), 0.3 mL deionized water, and 80 mL of methanol were mixed and then placed inside the autoclave. The autoclave was then sealed and the content degassed by flushing with a 1/1 mixture of CO/C_2H_4 at 0.5 MPa followed by depressurizing to atmospheric pressure. This was done three times. The autoclave was then brought to 90 ^oC before ethylene (pressurized to 2.25 MPa) was added followed by carbon monoxide (2.25 MPa). The total pressure in the reactor was 4.5 MPa and this was maintained throughout the entire reaction time by supplementing the reactor from a CO/C_2H_4 reservoir. The reaction ran for 1 hour at a stirring rate of 700 rpm. After cooling to room temperature a solid product was collected, filtered and washed three times with methanol and petroleum ether. The resulting white powder PK was dried in vacuum for approximately about 1 hour before being kept in an oven at 70 ^oC for 5 hours.

2.3 Amination of Polyketone

In a 100 mL round bottom flask equipped with a reflux condenser, 1,2-diaminopropane (1.53 mL, 0.018 mol) and triethylamine (6.97 mL, 0.05 mol) were added to a suspension of 1.0 g of polyketone (PK) in 50 mL of methanol. The reaction mixture was brought to reflux and left for 25 days at 100 ^oC. The product was filtered and washed with methanol and diethyl ether to remove the residual solvent and amine. Then, it dried under vacuum for 5 hours at 10^{-2} mbar and ambient temperature. The final product (PK-PDAP) is a light brown powder. The prepared polyamine (PK-PDAP) was found to be insoluble in water and common organic solvents except 1,1,1,3,3,3-hexafluoroisopropanol (HFIP).

2.4 Membrane casting

0.3 g of PK-PDAP were added to 7 mL of HFIP and stirred for 30 minutes at 40 ^{o}C. Then 120 mL of ammonium hydroxide vapor was bubbled directly into the solution by a syringe. The solution was homogenized by treatment in an ultrasonic bath (TRANSSONIC 46O/H) for 45 minutes at 40 ^{o}C before being left to stir over night at 40 ^{o}C. The solution was then cast onto a petri dish. A homogenous membrane (PK-PDAPm) was obtained and dried under vacuum at 40 ^{o}C for 24 hours. The thickness of the membranes ranged from 100-200 μm.

2.5 Methylation

PK-PDAPm was immersed in an excess amount of iodomethane in room temperature for 24 hours under fume hood. The methylated membrane was first removed from iodomethane residue, then thoroughly washed with deionized water and eventually dried at 40 ^{o}C under vacuum for 24 hours to obtain PK-PDAPm(I).

2.6 Anion Exchange

Anion exchange was carried out under a nitrogen atmosphere by soaking the methylated membrane (PK-PDAPm(I)) in solution of 1 M KOH for 1 hour. This was repeated three times with a fresh KOH solution each time. Then the membrane PK-PDAPm(OH) was washed with distilled water and stored under a nitrogen atmosphere. In order to evaluate stability of PK-PDAPm(OH) is immersed in a 2M NaOH solution and kept at 80°C.

Samples of membrane are then taken after 24, 40 and 64 hours and analysed using HR-TGA.

2.7 Instrumental methods

Elemental analysis was carried out using a FISONS EA-1108 CHNS-O instrument.

The iodine content of the PK-PDAPm(OH) was determined by inductively coupled plasma atomic emission spectroscopy (ICP-AES) using an ICP SPECTRO Arcos with EndOnPlasma torch. The analyses were performed using the emission lines λ(I) of 178.276 nm.

Modulated Differential Scanning Calorimetry (MDSC) analyses were performed using a MDSC 2920 Differential Scanning Calorimeter (TA Instruments) equipped with the LNCA low temperature attachment operating under a helium flux of 30 cm^3/min. The data were collected in the temperature range from -150 ^oC to 150 ^oC with a heating rate of 3 ^oC/min. The measurements were performed loading 3 mg of sample in an hermetically sealed aluminum pan.

High-Resolution Thermogravimetric analysis (HR-TGA) was carried out using a high-resolution modulated TGA 2950 (TA Instruments) thermobalance. A working N_2 flux of 100 cm^3/min was used. TGA measurements were collected from room temperature to 850 ^oC, using open platinum pans. The heating rate was varied dynamically during the ramp in response to the derivative of weight change from 50 to 0.001 ^oC/min. Sensitivity was set from 0.1 to 2%/min weight change. The balance resolution is 1μg.

Fourier Transform Infrared Spectroscopy (FTIR) was collected using a Nicolet

FT-IR Nexus spectrometer by averaging 1000 scans and a resolution of 4 cm^{-1} in the wavenumber range between 400 and 4000 cm^{-1}. UV-Vis measurements were performed using Perkin Elmer (Lambda 40). All absorption spectra were collected under identical conditions; scanning from 200 to 600 nm, at a rate of 120 nm/min.

Electrical spectra were measured with Broadband Electrical Spectroscopy (BES) in the frequency range from 30 mHz to 100 MHz using a Novocontrol Alpha-A Analyzer over the temperature range from -100 to 120 ^{o}C. The temperature was controlled using a homemade cryostat operating with an N_2 gas jet heating and cooling system. The membranes were sandwiched between two circular platinum electrodes inside a sealed cylindrical cell. The cell was closed in a glove-box filled with nitrogen.

3. Results and discussion

3.1 Elemental analyses

The chemical composition of all samples, as determined by elemental analysis (CHNS) and ICP-AEOS (iodine), is shown in Table 1.

The composition of PK synthesized in this work corresponds to theoretically expected stoichiometry. The negligible differences in C, H and O amounts are due to the presence of water traces. It was expected that the amination process took place by the reaction of two adjacent carbonyl groups of the polymeric chain with amine to form a pyrrole ring (see Fig. SI1 in supplementary Information). The amination process of polyketone led to a product (PK-PDAP) with about 5.3 wt% of nitrogen and this value did not vary significantly after the membrane preparation (PK-PDAPm). This N content is quite low and suggests the presence of a fraction of unreacted ketone groups in the

functionalized PK (PK-PDAP). Moreover, from the elemental analysis of PK-PDAP, it is possible to hypothesize the structure, defined in Scheme 1, with x/y about 5. This also accounts for the low methylation degree of PK-PDAPm(I) and PK-PDAPm(OH). In fact, only 10% of N present in the material was functionalized as quaternary groups (see table 1). Accordingly, these anionic membranes have a low concentration of mobile anion, although the experimental ion exchange capacity (IEC) of PK-PDAPmOH measured by back titration is comparable to that of commercial membranes [38, 39].

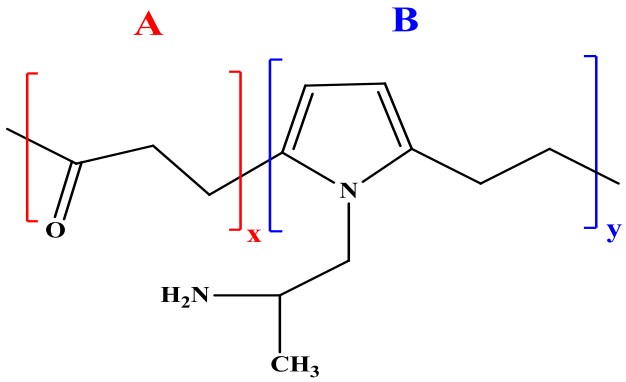

Scheme 1. Chemical structure of polyketone (A) and product of reaction of PK with 1,2-diaminopropane (B)

3.2 FT-IR studies

The FTIR spectra of the PK, PK-PDAP, PK-PDAPm, PK-PDAPm(I) and PK-PDAPm(OH) have been carried out and represented in Figure 1 (a-b). Assignments of peaks are made by correlative method and are shown in Table 2.

The vibration spectra of PK give rise to a strong peak observed at 1688 cm^{-1}, corresponded to the stretching vibration frequency of carbonyl (C=O) group [37, 40-41]. The various mode attributed to (stretching, bending, wagging and rocking) CH_2 are observed at 1405, 1331, 1258,1055, 831, 810 and 666 cm^{-1} [37, 40-43]. Bands at 591, 543 and 466 cm^{-1} correspond to the vibration of (CC=O) along PK chain and (CCC) polymer chain [37, 42, 43, 44]. The bending vibration of CH_3, due to terminal group of PK, is detected at 1351 and 1427 cm^{-1} [42,45]. In addition, the peaks at 2911 and 2947 cm^{-1} in Figure 1(a) correspond to the symmetric and antisymmetric vibration, respectively, of CH_2 [37, 40-42, 44, 45]. The peak at 3390 cm^{-1} is related to the stretching of OH, arising from keto–enol tautomerism [37,42,44,46]. This is in agreement with the presence of the shoulder at 1662 cm^{-1} attributed to the stretching vibration of C=C.

The modification of PK by amine leads to a decreased intensity of carbonyl (C=O) group at 1689 cm^{-1}, meantime new peaks are present in PK-PDAP spectra: a) a broad band at 754 cm^{-1} corresponding to the vibration of C-C out of plane in the pyrrole ring; b) a broad peak at 1567 cm^{-1} corresponding to the C=C stretching frequency [47] and assigned to the existence of pyrrole; c) a peak at 919 cm^{-1} due to the bending vibration out of plane of (=C-H) in the ring [30,40,41,43]; d) two shoulders visible at 1296 and 1076 cm^{-1} attributed to the C-N stretching vibration of the rings [45]. This analysis allows us to conclude that the reaction of 1,2-

diaminopropane with PK leads to formation of N-substituted pyrrole ring along in a chain having carbonyl groups.

In PK-PDAPm, the main peaks of PK-PDAP remain unchanged, but new features can be observed as effect of the molecular rearrangement occurred during the membrane preparation: a) a new peak at 726 cm^{-1} due to CH_2 bending of long chain-band [45], b) new peaks at 1173 and 1217 cm^{-1} corresponding to the C-N stretching vibration mode [44,45], c) a shift of (=C-H) out of plane bending vibration from 919 cm^{-1} to higher wavenumber (954 cm^{-1}).

In the spectra of PK-PDAPm(I), due to the methylation reaction, where a new carbon-amine bond is formed through the attack of amine to the electrophilic carbon of CH_3I, the C-N stretching vibration give rise to a new peak at 684 cm^{-1} and two weak shoulders at 1095 and 1291 cm^{-1} [44,45]. Some new peaks are also observed in the spectra of PK-PDAPm(I) including: a) peaks at 890 and 970 cm^{-1} due to (=C-H) out of plane bending vibration in the ring; b) a shift of (C=C) of aromatic ring (1567 cm^{-1}) to higher wavenumber (1590 cm^{-1}).

The IR spectra of PK-PDAPm(OH) show that the peaks due to C-N stretching vibration at 890 and 1095 cm^{-1} in the spectra of PKPDAPm(I) are shifted to 917 and 1089 cm^{-1}: this accounts for the anion exchange processes.

The detailed assignment of the spectra of materials here proposed is summarized in Figure 1 and Table 2.

3.3 UV-Vis Spectroscopy

The UV-Vis spectroscopy was carried out between 300 and 600 nm to define the molecular structure of the materials. The spectrum of PK-PDAP in HFIP solvent (Figure SI2) is shown in Figure 2. PK-DPAP exhibits absorption peaks at 325, 352 and 468 nm, which although weak, are in agreement with the values of N-substituted pyrrole rings found in literature [48,49].

3.4 Thermogravimetric Analysis

The thermal behaviour of PK, PK-PDAP, PK-PDAPm, PK-PDAPm(I) and PK-PDAPm(OH) measured by TGA under an inert atmosphere is shown in Figure 3 (a-b). TGA thermograms of all samples show a small weight loss (1-2%) below 200 ^{o}C caused by moisture evaporation. PK is stable up to 340 ^{o}C, when the first main weight loss of 14% appears due to intra-molecular and inter-molecular reactions accompanied by crosslinking and formation of heterocyclic compounds [42]. The second main weight loss of 50% occurs at 377 ^{o}C and is associated to the fragmentation of the molecular backbone with the formation of alcohols, as already reported for the ethylene–CO copolymers [42].

With respect to PK, the onset of thermal degradation of PK-PDAP occurs at lower temperatures and in three distinct regions: I) one at 215 ^{o}C is attributed to the loss of amine groups; II) the next one at 300 ^{o}C is tentatively assigned to the decomposition of the aminated nitrogen heterocycle; III) the main decomposition at temperature higher than 450 °C is due to degradation of polymeric backbone.

The thermal behaviour of PK-PDAPm is slightly different compared to PK-PDAP sample, because the multi decomposition events at higher temperature (T>300 °C) are very low, although three decomposition steps occur again: I) a first one (9%wt) at 215 °C

due to the loss of amine group; II) a second weight loss 8% occurred at 314 °C; III) the final main degradation at 377 °C with 35% of weight loss.

In the TG profiles of PK-PDAPm(I), beside the loss of amine group (I) and polymer backbone degradation (II), at low (200 °C) and high temperature (445 °C) respectively, also the cleavage of methylated group (III) was observed at 300 °C with 21% of weight loss. The TG profile of PK-PDAPm(OH) shows three decomposition steps: I) an initial step at 212 °C with 9 % weight loss, II) a second degradation at 280 °C with 16 % weight loss and III) the third degradation at 434 °C with a further 14 % weight loss.

3.5 DSC

The DSC thermograms of all samples showed multiple thermal transition events, related likely to the various domains composing the materials, as previously proposed and discussed. In the DSC curve of PK (Figure 4), the endothermic peak at 102 °C is identified as the α to β phase transition [25] typically of this material. These two crystalline phases correspond to two domains characterized by a different packing of polymer domains. This chain reorganization takes place by dipole interactions between neighboring carbonyl groups, which are closer in the alpha phase than in the β phase [50].

In accordance with the literature [25], the glass transition temperature of PK is not detected in this DSC profile. It has been reported elsewhere that the glass transition temperature of PK falls in a 5-20°C range and the magnitude of the transition is weaker for the copolymer (ethylene/CO) with respect the terpolymer (ethylene/propylene/CO). This is due to the low crystallinity of the terpolymer compared to that of the copolymer [25].

PK-PDAP shows two small endothermic peak at 41 (I) and 72 ^{o}C (II), respectively, which can be associated with the structural rearrangements. In the thermogram of polyamine membrane (PK-PDAPm), four transition phenomena can be distinguished at 10, 53, 69 and 124 ^{o}C. The transitions below 100 ^{o}C are attributed to the structural rearrangement of the fraction of polyamine structure of the polymer, whereas the peak at higher temperature corresponds to the order-disorder inter-chain cross-linking interactions [51,52].

The mDSC profiles of the dry and wet membranes in both the iodide and hydroxide form showed four transitions (I, II, III & IV) as shown in Figure 5. PK-PDAPm(I) in dry condition presents mainly one endothermic transition at about 120 °C, whereas in wet condition it shows an overlapping endothermic event peaking in 80-120 °C temperature range. This phenomenon is associated to the order-disorder transition attributed to the presence of chain cross-linking interactions. The transitions occurring at -75, -10 and 71 °C (I, II, III) and at -78, -20 and 34 °C (I, II, III) for dry and wet PK-PDAPm(I), respectively, correspond to the order-disorder molecular rearrangement and melting of nanometric domains. Analogously the DSC profiles of PK-PDAPm(OH) in both the conditions indicated some order-disorder molecular rearrangement, as well as melting of nano domains below 60 °C, followed by an endothermic peak at temperatures above 100 °C. This event, which is more evident in wet condition with a broad endothermic peak with maximum at 128 °C, is likely due to the elimination of water produced from the rearrangement of hydroxide anions.

3.6 Conductivity measurements

The conductivity of the iodide (PK-PDAPm(I)) and OH membrane (PK-PDAPm(OH)) in the dry and wet condition was tested by Broadband Electrical Spectroscopy (BES) in the temperature range of -100 / 120 °C and frequency range of 0.03 / 10^{7} Hz. The 2D spectra of real component of conductivity (σ') as function of frequency and temperature are shown in Figure 6. It is possible to observe that: a) the σ' of iodine membranes in dry and wet materials are higher than that of hydroxyl ones; b) as expected, the σ' values of wet membranes are higher than those of ionomer in dry conditions. (The imaginary and real parts of permittivity are shown in Figure SI3 and SI4, respectively, for dry and wet membranes.)

In wet membranes, the 2D spectra of σ' show as temperature increases: a) a shift of dielectric relaxations at higher frequency, b) the appearance of a electrode polarization (σ_{EP}), due to the accumulation of charge between sample and electrode, c) an enhancement of conductivity for T>0 due to the melting of water, which leads an increase on charge mobility, d) the presence of an inter-domains polarizations (σ_{IP}) [53] due to the accumulation of charge at the interfaces between domains with different permittivity present in the bulk membranes. These results are in accordance with the domains detected for DSC measurements previously discussed. In dry PK-PDAPm(I), the 2D spectra of σ' profiles show a dielectric relaxation at low temperature (T < 0°C) and an electrode polarization at higher temperatures (T > 0°C) [45], while in dry PK-PDAPm(OH), no electrode polarization is visible.

The highest conductivity of proposed materials is measured at 120°C, and for wet PK-PDAPm(I) and PK-PDAPm(OH) is $9x10^{-4}$ S cm^{-1} and $1x10^{-4}$ S cm^{-1}, respectively.

These values are comparable with those of other anionic membranes [11, 13, 54-56] (In Figure SI5 is shown the comparison of real conductivity vs. frequency/temperature between PK-PDAPm(OH) and AMVOH, a membrane prepared from the commercial Selemion AMV stability [57].) Moreover, the conductivity of the present new membranes can be even improved by rising the amine content of the modified polymer. Finally, the present membranes are promising because of their thermal stability. This last is gauged by measuring the mass loss that occurs during the thermal decomposition (Figure 7a), T_1: this is the thermal event occurring at *ca.* 260 °C associated with the loss of MeOH. After 60 h under alkaline conditions the mass loss is constant (approx. 6 w% as in (Figure 7b) indicating that under these conditions the membrane is stable.

In Figure 8, the overall conductivity (σ_T) as function of inverse of temperature is shown for dry and wet membranes of PK-PDAPm(I) (Figure 8a) and PK-PDAPm(OH) (Figure 8b), respectively (In Figure SI6 is shown the comparison of conductivity vs. 1/T between PK-PDAPm(OH) and AMVOH, a membrane prepared from the commercial Selemion AMV stability [57].) This kind of plot reveals the presence of four conductivity regions (I, II, III and IV) delimited by the thermal transitions measured by mDSC (see above): T_I, T_{II}, T_{III} and T_{IV}.

The overall conductivity (σ_T) is simulated with the Arrhenius-like equation [53, 58] (eq.1):

$$\sigma_T = A_\sigma \cdot \exp\left(-\frac{E_a}{RT}\right) \qquad \text{(eq. 1)}$$

where A_σ is related to the number of charge carriers, R is the universal gas constant, E_a is the activation energy, or by the Vogel–Fulcher–Tammann-like (VFT) equation [53, 59, 60, 61] (eq. 2):

$$\sigma_T = A_\sigma \cdot \exp\left(-\frac{E_{a,VTF}}{R(T-T_0)}\right) \qquad \text{(eq. 2)}$$

where $E_{a,VTF}$ is the pseudo-activation energy for conduction and T_0 is the thermodynamic ideal glass transition temperature, with boundary condition Tg - 55 ≤ T_0 ≤ Tg - 40 K [59]. The values of E_a and $E_{a,VTF}$ are reported in Table 3.

As expected, in dry membranes the conduction mechanism in regions I and II takes place owing to long range charge migration events between coordination site present in different neighboring chains (inter-chain hopping [15]) with an Arrhenius-like behaviour, while in the region III, the σ_T shows a VTF behavior. The VFT behaviour suggests that the migration of charge is coupled with the segmental motions of the host polymer matrix. The E_a value in these regions is about 1 kJ/mol. In wet membranes, the conductivity mechanism is VTF-like and it is expected that the charge migration occurs between delocalization body [12]. In the region III and IV, the $E_{a,VTF}$ values for PK-PDAPm(OH) are of the same order of magnitude and lower than those of PK-PDAPm(I).

Conclusion

Anion-exchange membranes were successfully prepared by chemical modification of polyketone with primary amine, followed by solution casting, methylation and ion exchange processes. Elemental analysis, FTIR and UV-Vis spectra revealed the presence of amine groups and polypirrole repeat units along the modified PK. The TGA thermogram of all compounds demonstrate a good thermal stability up to 200 °C. The ionic conductivity of the iodide and hydroxyl membranes in hydrated form can reach values as high as 9×10^{-4} S cm^{-1} at 120 °C and 5×10^{-4} S cm^{-1} at 90 °C, respectively. The obtained results indicated that, as the temperature increases, dielectric relaxations shift to higher frequency. Beside that, the electrode polarization appeared to be due to accumulation of charge between sample and electrode. In addition, the inter-domains polarizations can be seen at higher temperature because of the accumulation of charge at the interfaces between domains with different permittivity in the bulk membranes. The dielectric relaxation at low temperature ($T < 0°C$) and electrode polarization at higher temperature ($T > 0°C$) are responsible for the ionic conductivity of PK-PDAPm(I) in dry form, whereas in dry PK-PDAPm(OH), this is due to dielectric relaxation. The measurements of temperature dependence for PK-PDAPm(I) and PK-PDAPm(OH) in both wet and dry conditions showed four conductivity regions (I, II, III and IV), related with the thermal transitions measured by mDSC. In dry membranes the conduction mechanism of regions I and II follows an Arrhenius-like behaviour. The obtained results indicated that the relationship is non-linear for all regions since in the region III conductivity follows a VTF behavior. However, in wet membranes, the conductivity does not obey the Arrhenius rule.

The overall conductivities of PK-PDAPm(I) and PK-PDAPm(OH) are preliminary values, susceptible to being even improved by increasing N atoms in the membrane through an higher rate of conversion of carbonyl group of pristine PK into amine ones.

Acknowledgements

The author gratefully acknowledges University of Trento for allowing this research to be carried out. This work was conducted with support from “Progetto Strategico Maestra - From Materials for Membrane-Electrode Assemblies to Electric Energy Conversion and Storage Devices’” of The University of Padova Italy (V.D. PI).

References:

[1] V. Di Noto, T.A. Zawodzinski, A.M. Herring, G.A. Giffin, E. Negro, S. Lavina, Polymer electrolytes for a hydrogen economy. Int. J. Hydrogen Energy, 37 (2012) 6120-6131.

[2] G. Couture, A. Alaaeddine, F. Boschet, B. Ameduri,. Polymeric materials as anion-exchange membranes for alkaline fuel cells, Prog. Polym. Sci, 36 (2011) 1521-1557.

[3] J. Kim, T. Momma, T. Osaka, Cell performance of Pd–Sn catalyst in passive direct methanol alkaline fuel cell using anion exchange membrane, J. Power Sources, 189 (2009) 999–1002.

[4] N. Wagner, M. Schulze, E. Gülzow, Long term investigations of Silver cathodes for alkaline fuel cells, J. Power Sources, 127 (2004) 264–272.

[5] J.R. Varcoe, R.C.T. Slade, Prospects for alkaline anion-exchange membranes in low temperature fuel cells, Fuel Cells, 5 (2005) 187–200.

[6] J. Wind, R. Späh, W. Kaiser, G. Böhm, Metallic bipolar plates for PEM fuel cells, J. Power Sources, 105 (2002) 256–260.

[7] Y.J. Wang, J. Qiao, R. Baker, J. Zhang, Alkaline polymer electrolyte membranes for fuel cell applications, Chem.Soc.Rev, 42 (2013) 5768–5787.

[8] D. Chen, M.A. Hickner, E. Agar, E.C. Kumbur, Optimized anion exchange membranes for vanadium redox flow batteries, ACS Appl. Mater.Interfaces, 5 (2013) 7559–7566].

[9] Y. Leng, G. Chen, A.J. Mendoza, T.B. Tighe, M.A. Hickner, C.Y. Wang, Solid-state water electrolysis with an alkaline membrane, J.Am.Chem.Soc,134 (2012) 9054–9057.

[10] W. Garcia-Vasquez, L. Dammaka, C. Larchet, V. Nikonenko, N. Pismenskaya, D. Grande, Evolution of anion-exchange membrane properties in a full scale electrodialysis stack, Journal of Membrane Science, 446 (2013) 255–265.

[11] T.P. Pandey, H. N. Sarode, Y. Yang, Y. Yang, K. Vezzù, V. Di Noto, S. Seifert, D. M. Knauss, M. W. Liberatore, A. M. Herring, A highly hydroxide conductive, chemically stable anion exchange membrane, Poly(2,6 dimethyl 1,4 phenylene oxide)-*b*-Poly(vinyl benzyl trimethyl ammonium), for electrochemical applications, Journal of The Electrochemical Society, 163 (2016) 513-520.

[12] V. Di Noto, G.A. Guinevere, K. Vezzù, G. Nawn, F. Bertasi, T.-H. Tsai, A. Maes, S. Seifert, B. Coughlin, A. Herring, Interplay between solid state transitions, conductivity mechanism, and electrical relaxations in a [PVBTMA][Br]-b-PMB diblock copolymer

membrane for electrochemical applications, Phys Chem Chem Phys, 17 (2015) 31125-311139.

[13] T. P. Pandey, A. M. Maes, H. N. Sarode, B. D. Peters, S. Lavina, K. Vezzu, Y. Yang, S. D. Poynton, J. R. Varcoe, S. Seifert, M. W. Liberatore, V. Di Noto, A. M. Herring, Interplay between water uptake, ion interactions, and conductivity in an e-beam grafted poly(ethylene-co-tetrafluoroethylene) anion exchange membrane, Phys Chem Chem Phys, 17 (2015) 4367-4378.

[14] H. Sarode, M.A. Vandiver, Y. Liu, A.M. Maes, T.P. Pandey, S. Piril Ertem, T. Tsai, B. Zhang, D.C. Herbst, G.E. Lindberg, Y.-L. S. Tse, S. Seifert, V. Di Noto, E. B. Coughlin, Y. Yan, G.A. Voth, T.A. Witten, D. Knauss, M.W. Liberatore, A.M. Herring, Thin robust anion exchange membranes for fuel cell applications, ECS Trans, 64 (2014)1185-1194.

[15] G.A. Giffin, S. Lavina, G. Pace, V. Di Noto, Interplay between the structure and relaxations in selemion AMV hydroxide conducting membranes for AEMFC applications, J. Phys. Chem. C, 116 (2012) 23965-23973.

[16] D. Valade, F.d.r. Boschet, B. Améduri, Synthesis and modification of alternating copolymers based on Vinyl Ethers, Chlorotrifluoroethylene, and Hexafluoropropylene, Macromolecules 42 (2009) 7689–7700.

[17] H. Herman, R.C.T. Slade, J.R. Varcoe, The radiation-grafting of vinylbenzyl chloride onto poly (hexafluoropropylene-co-tetrafluoroethylene) films with subsequent conversion to alkaline anion-exchange membranes: optimisation of the experimental conditions and characterisation, Journal of Membrane Science 218 (2003) 147–163.

[18] J.R. Varcoe, R.C.T. Slade, E. Lam How Yee, S.D. Poynton, D.J. Driscoll, D.C. Apperley, Poly (ethylene-co-tetrafluoroethylene)-derived radiation-grafted anion-exchange membrane with properties specifically tailored for application in metal-cation-free alkaline polymer electrolyte fuel cells, Chemistry of Materials 19 (2007) 2686–2693.

[19] M.S. Huda, R. Kiyono, M. Tasaka, T. Yamaguchi, T. Sata, T., Thermal membrane potential across anion-exchange membranes with different benzyltrialkylammonium groups, Separation and Purification Technology 14 (1998) 95–10.

[20] Y. Wan, B. Peppley, K.A.M. Creber, V.T. Bui, E. Halliop, Quaternized-chitosan membranes for possible applications in alkaline fuel cells, J. Power Sources 185 (2008)183–187.

[21] E.S. Dragan, E. Avram, D. Axente, C. Marcu, Ion-exchange resins. III. Functionalization-morphology correlations in the synthesis of some macroporous, strong

basic anion exchangers and uranium-sorption properties evaluation, Journal of Polymer Science, Part A: Polymer Chemistry 42 (2004) 2451–2461.

[22] V. Di Noto, E. Negro, S. Polizzi, K. Vezzù, L. Toniolo, G. Cavinato, Synthesis studies and fuel cell performance of " core-shell" electrocatalysts for oxygen reduction reaction based on a PtNix carbon nitride "shell" and pyrolyzed polyketone nanoball "core" Int. J. Hydrogen Energy 39 (2014) 2812-2827.

[23] F. Ballauf, O. Bayer, L. Leichmann, (to Faberfabriken Bayer) G. Patent., 863 711, (1941).

[24] E. Drent, P.H.M. Budzelaar, Palladium-catalyzed alternating copolymerization of alkenes and carbon-monoxide, Chemical review, 96(2) (1996) 663-681.

[25] A. Sommazzi, F. Garbassi, Olefin-carbon monoxide copolymers, Prog. Polym. Sci, 22 (1997) 1547- 1605.

[26] J.T. Guo, Y. Ye, Sh. Gao, Y.K Feng, Synthesis of polyketone catalyzed by PD/C catalyst, Journal of Molecular Catalysis A: Chemical, 307 (2009) 121–127.

[27] W.P. Mul, H. Dirkzwager, A.A. Broekhuis, H.J. Heeres, A.J. van der Linden, A.G. Orpen, Highly active, recyclable catalyst for the manufacture of viscous, low molecular weight, CO-ethene-propene-based polyketone, base component for a new class of resins, Inorganica Chimica Acta 327(1) (2002) 147-159.

[28] C. Bianchini, A. Meli, Alternating copolymerization of carbon monoxide and olefins by single-site metal catalysis, Coordination Chemistry Reviews, 225 (2002) 35-66.

[29] B.L.Rivas, E.D. Pereira, I. Moreno-Villoslada, Water-soluble polymer–metal ion interactions, Prog. Polym. Sci. 28 (2003) 173-208.

[30] S. Liu, S.P. Armes, Recent advances in the synthesis of polymeric surfactant, Curr. Opin. Colloid Interface Sci. 6 (2001) 249-256.

[31] T. Radeva, Physical chemistry of polyelectrolytes, CRC Press, (2001).

[32] A.A. Zagorodni,. Ion exchange materials: properties and applications, 1st ed., Elsevier Science, (2006).

[33] A. Akelah, A. Moet, Functionalized polymers and their applications, 1st ed., Chapman and Hall, (1990).

[34] Y.Zhang, A. A. Broekhuis, Marc C. A. Stuart, F. Picchioni, Polymeric amines by chemical modifications of alternating aliphatic polyketones, Journal of Applied Polymer Science, 107 (2008) 262–271.

[35] C. Toncelli, A. Haijer, F. Alberts, A. A. Broekhuis,m and F. Picchioni, The green route from carbon monoxide fixation to functional polyamines: a class of high-performing metal ion scavengers, Ind. Eng. Chem. Res. 54 (2015) 9450−9457.

[36] G. Cavinato, L.Toniolo, Carbonylation of ethene catalysed by Pd(II)-Phosphine complexes, Molecules, 19 (2014)15116-15161.

[37] V. Di Noto , E. Negro , S. Polizzi, K. Vezzu , L. Toniolo , G. Cavinato, Synthesis, studies and fuel cell performance of "core-shell" electrocatalysts for oxygen reduction reaction based on a PtNix carbon nitride "shell" and a pyrolyzed polyketone nanoball "core, Int. J. Hydrogen Energy, 39 (2014) 2812-2827.

[38] H. Koshikawa, K. Yoshimura, W. Sinnananchi, T. Yamaki, M. Asano, K. Yamamoto, S. Yamaguchi, H. Tanaka, Y. Maekawa, Counter-Anion Effect on the Properties of Anion-Conducting Polymer Electrolyte Membranes Prepared by Radiation-Induced Graft Polymerization , Macromol. Chem.Phys. 214 (2013) 1756-1762.

[39] A. Jikihara, R. Ohashi, Y. Kakihana, M. Higa, K. Kobayashi, Electrodialytic transport properties of anion-exchange membranes prepared from poly(vinyl alcohol) and poly(vinyl alcohol-co-methacryloyl aminopropyl trimethyl ammonium chloride), Membranes 3 (2013) 1-15.

[40] R. Sulcis, F. Vizza, W. Oberhauser, F. Ciardelli, R. Spiniello, N.T. Dintcheva, Recycling ground tire rubber (GTR) scraps as high-impact filler of in situ produced polyketone matrix, Polym. Adv. Technol, (2014) 1060–1068.

[41] O. Ohsawa , K.H. Lee , B.S. Kim , S. Lee , I.S. Kim, Preparation and characterization of polyketone (PK) fibrous membrane via electrospinning, Polymer, 51 (2010) 2007-2012.

[42] S. De Vito, F. Ciardelli, E. Benedetti, and E. Bramanti, Thermal phase-transitions of carbon monoxide-ethylene alternating copolymer- a FTIR study, Polym. Adv. Tech.8 (1997) 53–62.

[43] H. Xia, Y. Hashimoto, T. Morita, T. Hirai, Formation of polyketone particle structure by hexafluoroisopropanol solvent evaporation and effects of plasticizer addition, Journal Of Polymer Science, Part B: Polymer Physics, 52 (2014) 887–892.

[44] The Handbook of Infrared and Raman Characteristic Frequencies of Organic Molecules, Lin-Vien & Colthup & Fateley & Grasselli. 1st ed., (1991).

[45] Introduction to spectroscopy. Donald L.Pavia, Gary M. lampman, George S. Kriz, 4th ed., (2009).

[46] A.I. Hamarneh, H.J. Heeres, A.A. Broekhuis , F. Picchioni, Extraction of Jatropha curcas proteins and application in polyketone-based wood adhesives, International Journal of Adhesion & Adhesives, 30 (2010) 615–625.

[47] E.B. Fox, T. Smith, T. K. Williamson, S.E. Kendrick, Aging effects on the properties of imidazolium, quaternary ammonium, pyridinium, and pyrrolidinium-based ionic liquids used in fuel and energy production, Energy & fuels, 27 (2013) 6355-636.

[48] D.N. Huyen, N.T. Tung, T.D. Vinh, N.D. Thien, Synergistic effects in the gas sensitivity of polypyrrole/single wall carbon nanotube composites, Sensors 12 (2012) 7965-7974.

[49] M.A. Chougule, Sh.G. Pawar, P.R. Godse, R. N. Mulik, Sh. Sen, V.B. Patil, Synthesis and characterization of polypyrrole (PPy) thin films, Soft Nanoscience Letters, 1(2011) 6-10.

[50] J.M. Lagaron, M.E. Vickers, A.K. Powell, N.S. Davidson, crystalline structure in aliphatic polyketones, Polymer, 41 (2000) 3011–3017.

[51] J. A. Mikroyannidis. Crosslinkable aromatic polyketones with maleimide pendent groups, Journal of Polymer Science Part A: Polymer Chemistry, 28 (3) (1990) 669–677.

[52] S. D. Mikhailenko, G. P. Robertson, M. D. Guiver, S. Kaliaguine, Properties of PEMs based on cross-linked sulfonated poly (ether ether ketone), Journal of Membrane Science,285 (1-2) (2006)306–316.

[53] V. Di Noto, G.A. Giffin, K. Vezzù, M. Piga, S. Lavina, Solid state proton conductors: properties and applications in fuel cells, in: P. Knauth, M.L. Di Vona (Eds.), solid state proton conductors: properties and applications in fuel cells, John Wiley & Sons, Chichester, 2012, pp. 109–183.

[54] O. Brylev, F. Alloin, M. Duclot, J.L. Souquet, J.Y. Sanchez, New family of anion conducting polymers. Synthesis and characterization Electrochim Acta 48 (2003)1953-1959.

[55] N.J. Robertson, I.V.H.A. Kostalik, T.J. Clark, P.F. Mutolo, H.D. Abrun, G.W. Coates, Tunable high performance cross-linked alkaline anion exchange membranes for fuel cell applications, J Am Chem Soc 132 (2010) 3400–3404.

[56] T.J. Clark, N.J. Robertson, I.V.H.A. Kostalik, E.B. Lobkovsky, P.F. Mutolo, H.D. Abrun, G.W. Coates, A ring-opening metathesis polymerization route to alkaline anion exchange membranes: development of hydroxide-conducting thin films from an ammonium-functionalized monomer, J Am Chem Soc 131 (2009) 12888–9.

[57] G.A. Giffin, S. Lavina, G. Pace and V. Di Noto, Interplay between the structure and relaxations in selemion AMV hydroxide conducting membranes for AEMFC applications J. Phys. Chem. C 2012, 116, 23965−23973.

[58] V. Di Noto, Zeolitic inorganic-organic polymer electrolyte based on oligo(ethylene glycol) 600 K_2PdCl_4 and $K_3Co(CN)_6$, J. Phys. Chem. B, 104 (2000) 10116-10125.

[59] V. Di Noto, A novel polymer electrolyte based on oligo(ethylen glycol) 600, K_2PdCl_4, and $K_3Fe(CN)_6$, J. Mater. Res. 12 (1997) 3393-3403.

[60] V. Di Noto, M. Vittadello, Mechanism of ionic conductivity in poly(ethylen glycol 400)/$(MgCl_2)_x$ polymer electrolytes: studies based on electrical spectroscopy, Solid State Ionics 147 (2002) 309-316.

[61] V. Di Noto, K. Vezzù, G. Pace, M. Vittadello, A. Bertucco, Effect of subcritical CO_2 on the structural and electrical properties of ORMOCERS-APE systems based on Zr and Al, Electrochim. Acta 50 (2005) 3904-3916.